

SPACE CHARGE STUDY OF THE JEFFERSON LAB MAGNETIZED ELECTRON BEAM*

S.A.K. Wijethunga^{†1}, J.R. Delayen¹, F.E. Hannon², G.A. Krafft^{1,2}, M.A. Mamun², M. Poelker²,
R. Suleiman², S. Zhang²,

¹Old Dominion University, Norfolk, VA 23529, USA

²Thomas Jefferson National Accelerator Facility, Newport News, VA 23606, USA

Abstract

Magnetized electron cooling could result in high luminosity at the proposed Jefferson Lab Electron Ion Collider (JLEIC). In order to increase the cooling efficiency, a bunched electron beam with high bunch charge and high repetition rate is required. We generated magnetized electron beams with high bunch charge using a new compact DC high voltage photo-gun biased at -300 kV with alkali-antimonide photocathode and a commercial ultrafast laser. This contribution explores how magnetization affects space charge dominated beams as a function of magnetic field strength, gun high voltage, laser pulse width and laser spot size.

INTRODUCTION

The proposed Jefferson Lab Electron Ion Collider (JLEIC) must provide ultra-high collision luminosity ($10^{34} \text{ cm}^{-2}\text{s}^{-1}$) to achieve the promised physics goals and this necessitates small transverse emittance at the collision point. Emittance growth can be reduced by the process called electron cooling, where the electron beam with temperature T_e is co-propagated with the ion beam traveling at the same velocity but with temperature T_i where $T_i > T_e$. The ion beam is “cooled” as a result of the Coulomb collisions and the transfer of thermal energy from ions to the electrons. Thermal equilibrium is reached when both the particles have the same transverse momentum.

The cooling rate can be significantly improved using a “magnetized electron beam” where this process occurs inside a solenoid field which forces electrons to travel with small helical trajectories that help to increase the electron-ion interaction time while suppressing the electron-ion recombination [1, 2]. However, the fringe radial magnetic field at the entrance of the solenoid creates a large additional rotational motion which adversely affects the cooling process inside the solenoid. In order to overcome this effect, the electron beam is created inside a similar field but providing a rotating motion in the opposite direction, so that the fringe field effects at the exit of the photo-gun and at the entrance of the cooling solenoid exactly cancel.

In order to have efficient cooling at JLEIC, the cooling electron beam must have high bunch charge, high repetition rate, and low temperature (low emittance and low energy spread). The high bunch charge requirement results in large space charge forces. In this paper, we present systematic measurements designed to study the space charge effect in magnetized electron beam especially, how magnetization affect the space charge current limitations as a function of gun high voltage, laser pulse width and laser spot size.

EXPERIMENTAL SETUP

The experimental beamline consists of gun high voltage chamber, photocathode preparation chamber, cathode solenoid, green laser, three fluorescent YAG screens, harp, few focusing solenoids and beam dump. A schematic diagram of the beamline is shown in Fig. 1.

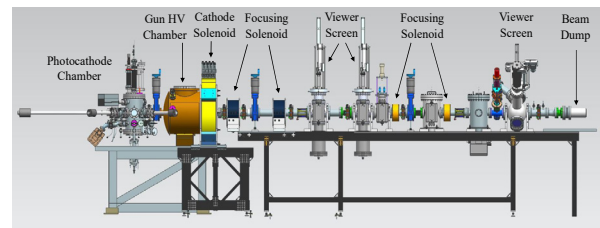


Figure 1: The diagnostic beamline.

The compact gun high voltage chamber includes an inverted insulator and spherical cathode electrode operating at or below -300 kV. The cathode-anode gap is 9 cm and the anode aperture is 2 cm. A load-lock type photocathode deposition chamber was installed behind the gun high voltage chamber to manufacture the photocathodes. For this experiment a bi-alkali-antimonide (K_2CsSb) photocathode made on GaAs substrate was used. The active area was limited to 3 mm radius and the typical quantum efficiency (QE) was in the range of 5-8% with 523 nm laser. A commercial ultrafast laser with pulse duration less than 0.5 ps, 20 μJ pulse energy, operating at 50 kHz pulse repetition rate and 1030 nm wavelength (NKT Origami) was used as the laser source for the experiment. The IR beam was converted to 515 nm using a BBO crystal. The laser spatial and temporal profiles were Gaussian. To explore parameter space, the laser beam size at the photocathode was varied and the temporal pulse width was varied using a pulse stretcher built with diffraction gratings. The magnetic field at the photocathode was provided by a solenoid magnet designed to fit at the front of the gun chamber, 0.2 m from the

* Authored by Jefferson Science Associates, LLC under U.S. DOE Contract No. DE-AC05-06OR23177. Additional support comes from Laboratory Directed Research and Development program. The U.S. Government retains a non-exclusive, paid-up, irrevocable, world-wide license to publish or reproduce this manuscript for U.S. Government purposes.

[†] wwije001@odu.edu

cathode. The magnet operates at a maximum current of 400 A to provide up to 0.1514 T at the photocathode. The diagnostic beam line extends to 4.5 m from the photocathode with different beam pipe aperture sizes range from 1-5 cm radii. There are two fluorescent YAG screen-slit combinations at 1.5 and 2.0 m, and one YAG screen at 3.75 m. Additionally, there are four focusing solenoids at 0.49, 1.01, 2.35 and 2.94 m and several steering dipole magnets [3].

THEORETICAL BACKGROUND

The emittance associated with the magnetized electron beam is given by [4],

$$\varepsilon_{tot} = \sqrt{\varepsilon_u^2 + \varepsilon_d^2} \quad (1)$$

where ε_u is the uncorrelated emittance which mainly represent the thermal emittance and ε_d is the correlated emittance (drift emittance) which represents the magnetization of the electron beam,

$$\varepsilon_d = \frac{eB_0\sigma^2}{8m_e c} \quad (2)$$

where B_0 and σ^2 are the magnetic field and laser spot size at the cathode, c is the speed of light, e and m_e are the electron charge and mass, respectively. Thus, the magnetic field at the cathode can generate canonical angular momentum, which in effect increases the correlated emittance of the electron beam [5].

Space charge forces describe the Coulomb repulsive forces that result from an accumulation of charge within a region. Space charge forces at high intensity accelerators/colliders can degrade the beam quality and cause instabilities. Space charge forces acting on a charge inside a Gaussian charge distribution, travelling with relativistic velocity is given by,

$$F_r(r, z) = \frac{q}{2\pi\epsilon_0\gamma^2} \frac{q_0}{\sqrt{2\pi}\sigma_z} e^{(-z^2/2\sigma_z^2)} \left[\frac{1 - e^{(-r^2/2\sigma_r^2)}}{r} \right] \quad (3)$$

where q_0 is the bunch charge, σ_z and σ_r are the longitudinal and transverse rms beam sizes respectively [6]. Since the transverse space charge force is inversely proportional to the bunch transverse dimension (Eq. (3)), for a non-magnetized electron beam, the bunch transverse dimension is small and the charge density is intense, hence the nonlinear space charge force can have huge effect during acceleration from low to higher energy and during the long drift. This would cause emittance growth beyond the specifications required for electron cooling. For a magnetized electron beam, the transverse size is set by the beam's correlated emittance which is much larger and thus the space charge effect is minimal.

Electrons within the cathode/anode gap can limit further emission of electrons from the surface of the photocathode due to space charge forces. This is known as the space charge current limitation [5, 7]. In this paper we investigate whether the space charge current limitation depends on the magnetization of the electron beam.

EXPERIMENTAL METHOD

Average beam current was measured at the dump by changing the laser power at the photocathode for different cathode solenoid currents (0, 100, 200 A). This procedure was repeated using a variety of laser spot sizes at the cathode (1.54, 1.00, 0.50, and 0.25 mm), laser pulse widths (120, 70, 1 ps) and gun voltages (200, 150, 100 kV), for magnetized and non-magnetized beam. Photocathode QE is the ratio of emitted electrons and incident photons, given by,

$$QE = \frac{hc I}{\lambda e P} \times 100\% = \frac{124 I}{\lambda P} \% \quad (4)$$

where P (W) is the incident laser power, I (mA) is the measured average current, λ is the laser wavelength (515 nm), h is Planck's constant (6.626×10^{-34} Js), e is the electron charge (1.602×10^{-19} C), and c is the speed of light (2.998×10^8 m/s). Bunch charge was determined by dividing the measured current by the repetition rate. In addition, laser pulse energy was calculated by dividing the laser power by the repetition rate.

MEASUREMENTS ANALYSIS

Fig. 2 shows the extracted charge and apparent QE as a function of laser pulse energy for different cathode solenoid currents. For each cathode solenoid current, QE falls rapidly with increasing laser power, implying that we have reached the space charge limitations immediately, mainly due to the relatively low gun voltage and shorter laser pulse width. Furthermore, the space charge limit is reached at ~ 0.3 nC and increased for a maximum extracted charge of 0.7 nC. We also see a notable dependence of the space charge current limitations on magnetization at small pulse energies. However, the charge beyond ~ 0.3 nC is likely to originate from the edge of the Gaussian laser profile. Also, we believe that the oscillatory behavior seen at higher pulse energies likely stems from beam loss. The limited beamline aperture and insufficient strength of the focusing solenoids prevent clean transportation of the beam to the dump.

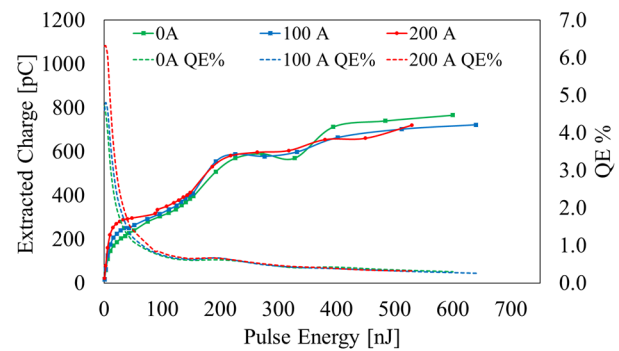


Figure 2: Extracted charge vs laser pulse energy and corresponding QE% for 0, 100 and 200 A cathode solenoid currents (225 kV, 50 kHz, 75 ps (FWHM), 1.64 mm (rms)).

Figure 3 shows how the space charge limit varies with the gun high voltage for magnetized and non-magnetized beam. These plots show the expected results namely, higher gun voltage permit the delivery of higher bunch

Any distribution of this work must maintain attribution to the author(s), title of the work, publisher, and DOI
 Content from this work may be used under the terms of the CC BY 3.0 licence © 2019.

charge beam. However, there is a less notable dependence of the space charge limitations on magnetization.

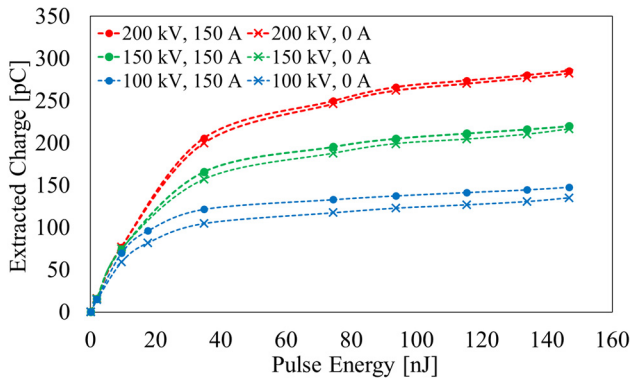


Figure 3: Extracted charge vs laser pulse energy variation with different gun high voltage for magnetized and non-magnetized beam (50 kHz, 1 ps (FWHM), 1.54 mm (rms)).

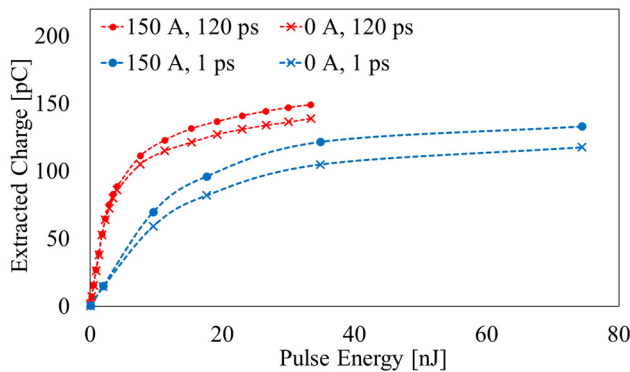


Figure 4: Extracted charge vs laser pulse energy variation with laser pulse width for magnetized and non-magnetized beam (100 kV, 50 kHz, 1.54 mm (rms)).

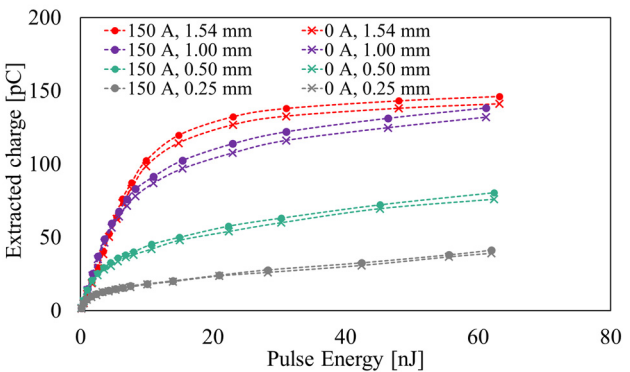


Figure 5: Extracted charge vs laser pulse energy variation with laser spot size for magnetized and non-magnetized beam (100 kV, 50 kHz, 70 ps (FWHM)).

Fig. 4 and Fig. 5 show how the space charge limit varies with the laser pulse width and laser spot size at the cathode for magnetized and non-magnetized beams respectively. Both agree with the space charge force equation (Eq. (3)): by increasing the bunch dimensions, space charge forces can be suppressed leading to an increase in the extracted

charge. However, both plots show a less notable dependence of the space charge current limitations on magnetization.

CONCLUSION

In summary, we used Jefferson Lab's -300 kV photo-gun and beamline to investigate the space charge effect in magnetized electron beam. A new laser source was installed specifically for this experiment which was capable of delivering nC bunch charge (high power and varying repetition rate up to 50 kHz) with low average current. Measurements were taken by varying the laser power and tracking the average current at the dump for different cathode solenoid currents. We repeated these measurements for different gun high voltages, laser spot sizes and laser pulse widths. Results showed that there is less notable dependence of the space charge current limitations on magnetization. In addition, the space charge current limitations can be reduced by using a higher gun voltage with larger laser spot size at the cathode and longer pulse width, regardless of the beam been magnetized. My future work will involve GPT (General Particle Tracer) simulations on optimizing the gun geometry, beam line components, solenoid settings to ensure maximum charge extraction to the dump, add more Faraday cups to the beamline to measure the current leaving the photocathode and track the beam loss throughout the beamline and perform more beam based measurements with the modified beamline to achieve the JLEIC requirements.

REFERENCES

- [1] Y. Derbenev and A. Skrinsky, "Magnetization effect in electron cooling," *Fiz. Plazmy*, vol. 4, p. 492, 1978; [*Sov.J. Plasma Phys.* vol. 4, p. 273, 1978.].
- [2] R. Brinkmann, Y. Derbenev and K. Flöttmann, "A low emittance flat-beam electron source for linear colliders," *Phys. Rev. ST Accel. Beams*, vol. 4, p. 053501, 2001.
- [3] S. Zhang *et al.*, "High Current High Charge Magnetized and Bunched Electron Beam from a DC Photogun for JLEIC Cooler", in *Proc. 10th Int. Particle Accelerator Conf. (IPAC'19)*, Melbourne, Australia, May 2019, pp. 2167-2170.
- [4] K.-J. Kim, *Phys. Rev. ST Accel. Beams*, vol. 6, 104002, 2003.
- [5] M. Reiser, *Theory and Design of Charged Particle Beams*, Germany, Wiley-VCH, 2008.
- [6] M. Ferrario, M. Migliorati, and L. Palumbo, "Space charge effects," in *Proc. of the CAS-CERN Accelerator School*, p. 331, 2014.
- [7] I. Langmuir, "The effect of space charge and residual gases on thermionic currents in high vacuum," *Phys. Rev.* 2, 1913.